



# Isophthaloyl-Based Selective Fluorescence Receptor for Zn (II) Ion in Semi-Aqueous Medium

N. B. Khadke<sup>1</sup> · A. A. Patil<sup>2</sup> · D. Y. Patil<sup>2</sup> · A. V. Borhade<sup>2</sup>

Received: 29 August 2018 / Accepted: 6 May 2019 / Published online: 15 July 2019  
© Springer Science+Business Media, LLC, part of Springer Nature 2019

## Abstract

A novel Isophthaloyl-based symmetrical (12E,21E)-N1',N3'-bis(2-hydroxybenzylidene) isophthalohydrazide, receptor (1) was synthesized and characterized using various spectroscopic technique. The reorganization ability of receptor (1) was evaluated in semi-aqueous medium and shows significant enhancement in fluorescence intensity for Zn (II) ion over various metal ions in CH<sub>3</sub>CN:H<sub>2</sub>O (1:1, v/v). The 1:2 binding stoichiometry between receptor (1) and Zn (II) ion was established using Job's plot and the proposed complex structure was calculated by applying Density Functional Theory (DFT) method. The binding constant ( $K_a$ ) of receptor (1) with Zn (II) ion was established with the Benesi-Hildebrand plot, Scatchard and Connor's plot and the values are  $1.00 \times 10^4 \text{ M}^{-1}$ ,  $1.05 \times 10^4 \text{ M}^{-1}$  and  $1.05 \times 10^4 \text{ M}^{-1}$  respectively. The limit of detection (LOD) and limit of quantification (LOQ) of receptor (1) and Zn (II) ion was 0.292  $\mu\text{M}$  and 0.974  $\mu\text{M}$  respectively. The binding mode was due to photo-induced electron transfer (PET) and the coordination of Zn (II) ion with C = N hydroxyl group of receptor (1). Electrochemical analysis of metal free receptor (1) and with Zn (II) ion also confirmed the formation of complex.

**Keywords** Fluorescent chemosensor · Zn (II) detection · Binding constant · DFT

## Introduction

A selective fluorescence chemosensor for biologically active metal ions is topic of growing interest in supramolecular chemistry due to their active role in many biological, physiological and environmental processes [1–4]. Along with various transition metal ions, biologically important Zn (II) has received considerable attention [5, 6]. Zinc is the second most abundant and essential transition metal after iron in the human body, and known to play a role in various biological processes such as catalytic co factor of many enzymes, stabilization of protein structure, neurotransmission, signal transduction, cellular

apoptosis and modulation of interactions between macromolecules [7–12]. Minute quantity of Zn (II) is essential for living organisms, but either deficiency or excessive amount can have various detrimental effects [13, 14]. According to WHO, its daily requirement for adult men is 15–20 mg/day and recent studies on humans, drinking-water containing zinc at levels above 3–5 mg/L may not be acceptable to consumers [15, 16]. Excessive Zn (II) ion will cause imbalance in cellular process, resulting in neurological diseases such as Menkes and Wilson disease, amyotrophic lateral sclerosis (ALS), Alzheimer's disease (AD), Parkinson's disease, prostate cancer disease, diabetes, infantile diarrhoea, epilepsy and also reduce the soil microbial activity resulting in phototoxic effect [17–24]. Therefore, development of a fluorescent chemosensor selective to Zinc is of considerable interest [25, 26].

The sensing and quantification of magnetic-silent Zn (II) ion is challenging task because detection of Zn (II) was not possible by common analytical technique such as nuclear magnetic resonance (NMR), Mossbauer spectroscopy and electron paramagnetic resonance (EPR) spectroscopy [27, 28]. Therefore, the development of analytical method for the sensitive and selective determination of Zn (II) ion in various biological and environment sample is extremely desirable [29, 30]. So the fluorescence spectroscopy technique was used for detection

**Electronic supplementary material** The online version of this article (<https://doi.org/10.1007/s10895-019-02385-1>) contains supplementary material, which is available to authorized users.

✉ A. V. Borhade  
ashokborhade2007@yahoo.co.in

<sup>1</sup> Science Department, Government Residential Women's Polytechnic College, Latur 413512, India

<sup>2</sup> Department of Applied Science and Mathematics, K. K. W Institute of Engineering Education and Research, Nashik, 422003, India

of Zn (II) ion due to its many advantageous as high selectivity and sensitivity [31, 32].

In the present study, we report a simple Isophthaloyl-based highly selective and sensitive fluorescent receptor for Zn (II) ion in presence of various metal ions such as  $\text{Ag}^+$ ,  $\text{Al}^{3+}$ ,  $\text{Ca}^{2+}$ ,  $\text{Cd}^{2+}$ ,  $\text{Co}^{2+}$ ,  $\text{Cu}^{2+}$ ,  $\text{Fe}^{3+}$ ,  $\text{Hg}^{2+}$ ,  $\text{K}^+$ ,  $\text{Mg}^{2+}$ ,  $\text{Na}^+$  and  $\text{Ni}^{2+}$  in  $\text{CH}_3\text{CN}:\text{H}_2\text{O}$  (1:1, v/v). The binding constant and stoichiometry was computed with the Benesi–Hinderbrand plot and Job's plot respectively. The details characteristics of Receptor (1) have been investigated by  $^1\text{H}$  NMR,  $^{13}\text{C}$  NMR, LC-MS and quantum mechanical calculations at the level of density functional theory.

## Experimental

### Chemicals and Instrumentation

All chemicals were purchased from sigma-Aldrich company. All solvents and reagents used are of analytical grade and used directly without purification. The UV-Vis spectra were obtained on Shimadzu UV 2450 spectrophotometer. Fluorescence was recorded on Perkin Elmer model LS45 fluorescence spectrophotometer using a 1 cm path length quartz cuvette and 5 nm slit width. The fluorescence spectra were recorded from 400 nm to 700 nm at 390 nm excitation wavelength. Cyclic voltametric (CV) measurements of the compounds in  $\text{CH}_3\text{CN}$  were conducted using K-Lyte 1.2 series electrochemical analyser at room temperature. The electrolytic cell comprises three electrodes, Pt as working electrode, Pt mesh auxiliary electrode and Ag/AgCl as reference electrode (3 M KCl) separated from the sample solution by a salt bridge. The infrared spectra were recorded on Shimadzu IR affinity spectrophotometer using KBr.  $^1\text{H}$  NMR spectra were recorded on a 400 MHz spectrometer using tetramethylsilane (TMS) as an internal standard.  $^{13}\text{C}$  NMR spectrums were recorded on a 400 MHz spectrometer in D6-DMSO. Mass spectrums were obtained on water Q-TOF micro mass (LC-MS).

### Synthesis of Receptor (1)

#### Synthesis of Isophthaloyl Dihydrazide

Synthesis was carried out using 203 mg (1.0 mmol) Isophthaloyl dichloride dissolved in 5 ml of dry methanol along with catalytic amount of triethylamine and 0.12 ml (2.2 mmol) hydrazine hydrate was added drop wise with continuous stirring at room temperature for 18 h gives Isophthaloyl dihydrazide. Yield 84%, m.p. 222–5 °C,  $^1\text{H}$  NMR (DMSO- $d_6$ , 400 MHz,  $\delta$  in ppm)  $\delta$ : 9.82 s (2H, –NH–); 8.24 t (H, –CH– Ar); 7.91 m (H, –CH– Ar); 7.51 t (H, –CH– Ar); 4.53 s (4H, –NH<sub>2</sub>) Fig. S1;  $^{13}\text{C}$  NMR (DMSO- $d_6$ , 100 MHz, in ppm): 165.41 (–CONH–); 133.49 (Ar); 129.26 (Ar); 128.40 (Ar); 126.00 (Ar) Fig. S2.

### Synthesis of (12E, 21E)-N1',N3'-Bis(2-Hydroxybenzylidene) Isophthalohydrazide

0.25 ml (1.02 mmol) of salicylaldehyde added drop wise to the 200 mg (1.02 mmol) of Isophthaloyl dihydrazide dissolved in 25 ml of methanol with catalytic amount of acetic acid, stirred at room temperature for 10–12 h gives 1,3-phenylenedi(carbonyl hydrazone) i.e. Receptor (1). The precipitate was filtered, washed with methanol and dried under vacuum for 24 h (recrystallized from methanol) Yield 81%, m.p. >270 °C.  $^1\text{H}$  NMR (DMSO- $d_6$ , 400 MHz,  $\delta$  in ppm):  $\delta$  6.87–8.56 (m, 12H, ArH), 8.64 (s, 2H, N=CH), 11.34 (s, 2H, NH), 12.25 (s, 2H, OH) Fig. S3;  $^{13}\text{C}$  NMR (DMSO- $d_6$ , 400 MHz, in ppm): 162.16 (–CONH–), 157.75 (–CH=N), 149.34 (–C–OH), 133.03 (Ar), 131.11 (Ar), 130.84 (Ar), 129.95 (Ar), 128.47 (Ar), 126.94 (Ar), 118.97 (Ar), 118.11 (Ar), 116.35 (Ar) Fig. S4; IR (KBr)  $\nu(\text{cm}^{-1})$ : 3309.85 (OH), 3078.39 (NH), 1666.50 (–NH–C=O), 1620.21 (C=O), 1573.91 (C=N), 1280.73 (N=CH) Fig. S5; Mass LC-MS (ESI)  $m/z$  calc. For  $\text{C}_{22}\text{H}_{18}\text{N}_4\text{O}_4$ : 403.40112 [ $\text{M} + \text{H}$ ]<sup>+</sup>, found: 403.14220 [ $\text{M} + \text{H}$ ]<sup>+</sup> Fig. S7.

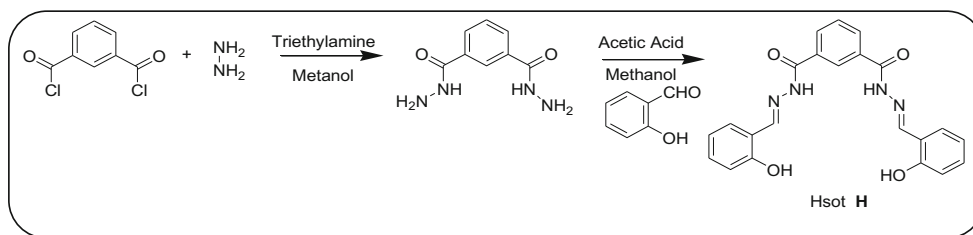
### Sample Preparation for Photo Physical Measurement

All the stock and working solutions were prepared in double distilled water and analytical grade acetonitrile. The nitrate salts of  $\text{Ag}^+$ ,  $\text{Al}^{3+}$ ,  $\text{Ca}^{2+}$ ,  $\text{Cd}^{2+}$ ,  $\text{Co}^{2+}$ ,  $\text{Cu}^{2+}$ ,  $\text{Fe}^{3+}$ ,  $\text{Hg}^{2+}$ ,  $\text{K}^+$ ,  $\text{Mg}^{2+}$ ,  $\text{Na}^+$ ,  $\text{Ni}^{2+}$  and  $\text{Zn}^{2+}$  were used to prepare the stock solutions with concentration  $1 \times 10^{-3}$  M in water. Synthesized receptor (1) was dissolved in mixed solution of  $\text{CH}_3\text{CN}:\text{H}_2\text{O}$  (1:1, v/v) to give stock solution with concentration  $1 \times 10^{-2}$  M. The stock solutions were used after appropriate dilution.

## Results and Discussion

### Fluorescence Spectral Measurement

In the present study receptor (1) was synthesized according to Scheme 1. The photo-physical properties of receptor (1) were discussed in detail. The photo-physical properties such as cation recognition ability of receptor (1) ( $1 \times 10^{-5}$  M) was studied in  $\text{CH}_3\text{CN}:\text{H}_2\text{O}$  (1:1, v/v) for various metal ions ( $\text{G} = \text{Ag}^+$ ,  $\text{Al}^{3+}$ ,  $\text{Ca}^{2+}$ ,  $\text{Cd}^{2+}$ ,  $\text{Co}^{2+}$ ,  $\text{Cu}^{2+}$ ,  $\text{Fe}^{3+}$ ,  $\text{Hg}^{2+}$ ,  $\text{K}^+$ ,  $\text{Mg}^{2+}$ ,  $\text{Na}^+$ ,  $\text{Ni}^{2+}$  and  $\text{Zn}^{2+}$ ) ( $1 \times 10^{-4}$  M) by fluorescence spectroscopy. Receptor (1) bearing imine- N and hydroxyl–OH are well known chelating group for transition metal ions. The possible binding mechanism is based on two fundamental principles of photo induced electron transfer (PET) and intra molecular charge transfer (ICT).

**Scheme 1** Synthetic procedure for receptor (1) (Host **H**)

## Sensitivity and Selectivity

The fluorescence spectrum of receptor (1) was recorded at excitation wavelength 390 nm. Most of the metal does not show significant change in fluorescence emission intensity except Zn (II) ion shown in Fig. 1a. It was clearly revealed that the receptor (1) was highly sensitive for Zn (II) ion over other surveyed metal ions. The Zn (II) shows significant enhancement in fluorescence emission intensity of receptor (1) and slight blue shift ( $\Delta = 11$  nm) and is shown in Fig. 1b.

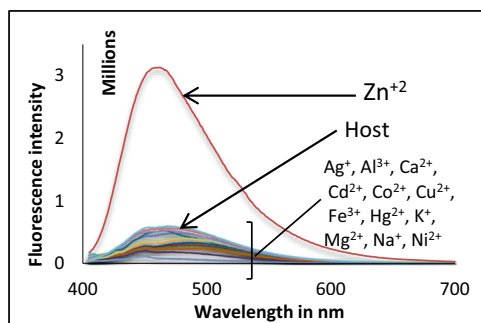
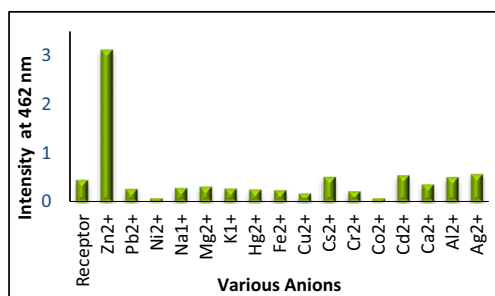
Notwithstanding sensitivity, selectivity is important phenomenon where receptors potential is validated. In order to validate the selectivity of receptor (1) towards Zn (II) ion, competitive experiments were carried out by addition of 1 equivalent of Zn (II) to the receptor (1) in presence of 1 equivalent of other metal ion such as of  $\text{Ag}^+$ ,  $\text{Al}^{3+}$ ,  $\text{Ca}^{2+}$ ,  $\text{Cd}^{2+}$ ,  $\text{Co}^{2+}$ ,  $\text{Cu}^{2+}$ ,  $\text{Fe}^{3+}$ ,  $\text{Hg}^{2+}$ ,  $\text{K}^+$ ,  $\text{Mg}^{2+}$ ,  $\text{Na}^+$  and  $\text{Ni}^{2+}$  as shown in Fig. 2a. This result showed no significant change in the emission intensity of receptor (1), indicating receptor (1) has high selectivity towards

Zn (II) ion in the presence of various competing metal ions. Thus receptor (1) could be used as selective fluorescence sensors for Zn (II) ion detection over the other cations.

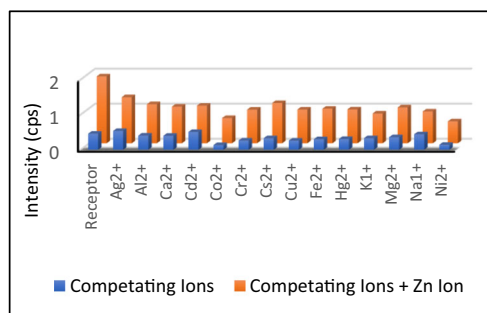
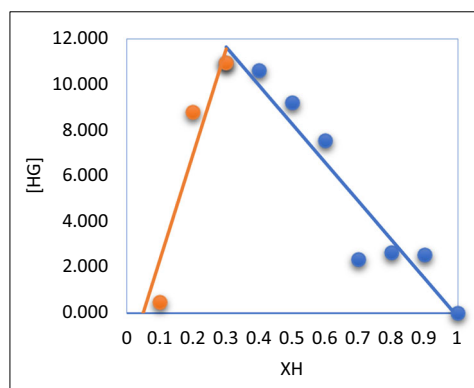
## Binding Stoichiometry and Binding Constant ( $K_d$ )

The binding stoichiometry was determined by Job's plot (continuous variation method) [33]. Figure 2b shows the Job' plot between  $[\text{HG}]$  and  $([\text{H}]/([\text{H}] + [\text{G}]))$ , where the total molar concentration of host and guest was constant and molar fraction of host was continuously varied. The  $[\text{HG}]$  is concentration of complex calculated as  $[\text{HG}] = (\text{F} - \text{F}_0)/\text{F}_0 \times [\text{H}]$ . The maximum fluorescence intensity at a 0.3 M fraction indicated the formation of a 1:2 (host:guest) i.e. receptor (1) and Zn (II) ion complex.

Fluorescence titration of receptor (1) ( $2 \text{ ml } 1 \times 10^{-5} \text{ M}$ ) with the successive addition of Zn (II) ( $1 \times 10^{-4} \text{ M}$ ,  $0 \rightarrow$

**a****b**

**Fig. 1** Fluorescence intensity of receptor (1) ( $1 \times 10^{-5} \text{ M}$ ,  $\lambda_{\text{ex}} = 390 \text{ nm}$ ) **a**) upon addition of various metal ions ( $1 \times 10^{-4} \text{ M}$ ) in  $\text{CH}_3\text{CN}:\text{H}_2\text{O}$  (1:1, v/v) **b**) at wavelength 462 nm

**a****b**

**Fig. 2** **a** Interference studies of various metal ions (1 equivalent) in presences of Zn (II) ion at 462 nm. **b** Job's plot for showing 1:2 stoichiometry of receptor (1) and Zn (II) ion (host and guest)

1 ml, 0 → 5 equivalents) was performed. The incremental addition resulted in increased in emission band at 462 nm in CH<sub>3</sub>CN:H<sub>2</sub>O (1:1, v/v) which is depicted in Fig. 4. The changes in the fluorescence intensity at 462 nm were used to evaluate the binding affinity of receptor (1) and Zn (II) ions. The binding constant ( $K_a$ ) was calculated by using Benesi-Hildebrand [34] Eq. (1), Scatchard [35] Eq. (2) and Connor's linear fitting equation [36] Eq. (3).

$$1/(F-F_0) = 1/(F_\infty-F_0)Ka[G] + 1/(F_\infty-F_0) \quad (1)$$

$$(F-F_0)/[G] = (F_\infty-F_0)Ka - (F-F_0)Ka \quad (2)$$

$$(1-F/F_0)/[G] = Ka(F/F_0) - \alpha Ka \quad (3)$$

Using above equations, graphs obtained were illustrated in Fig. 3a–c, Where  $F_0$  is the fluorescence intensity receptor (1),  $F$  is the fluorescence intensity with the Zn (II) ion and  $[G]$  is the concentration of guest Zn (II) ion. The stability constant ( $K_a$ ) value obtained from the Benesi–Hildebrand, Scatchard and Connor's fitting plot was in concord and value was found to be  $(1.025 \pm 0.025) \times 10^4 \text{ M}^{-1}$ .

#### Limit of Detection (LOD) and Limit of Quantification (LOQ)

Fluorescence titration results were used for calculating limit of detection (LOD) and limit of quantification (LOQ). The fluorescence emission intensity at 390 nm was plotted against the concentration of Zn (II) ion to obtain the slope shown in Fig. 4. The limit of detection (LOD) and limit of quantification (LOQ) of receptor (1) evaluated according to the IUPAC 3  $\sigma$  and 10  $\sigma$  method respectively [37].

$$\text{Limit of detection (LOD)} = 3S_b/m$$

$$\text{Limit of quantification (LOQ)} = 10S_b/m;$$

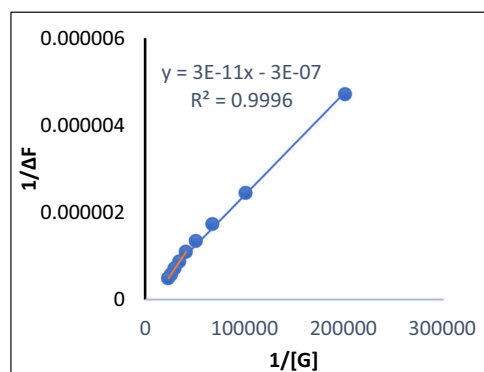
$S_b$  = standard deviation of blank,  $m$  = slope of regression line.

The LOD and LOQ of receptor (1) with Zn (II) ions were 0.292  $\mu\text{M}$  and 0.974  $\mu\text{M}$ .

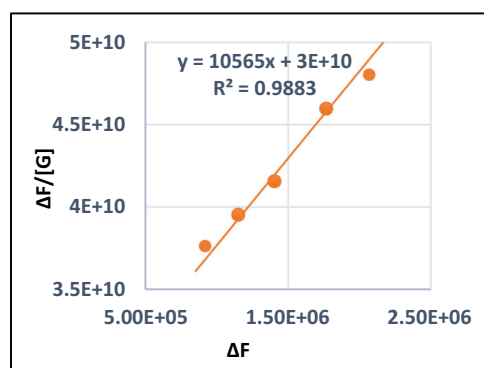
The recognition behaviour of receptor (1) with Zn (II) ion was further confirmed by FT-IR spectroscopy. IR of only receptor (1) showed a broad band at 3310  $\text{cm}^{-1}$  which assigned for (OH) group which disappear in complex of Zn (II) with receptor (1) showed in Fig. S5 and S6 respectively.

#### Density Functional Theory (DFT)

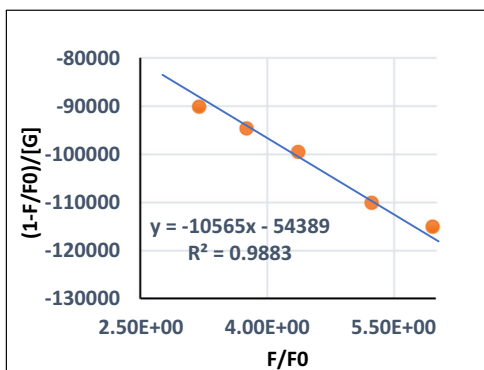
The binding behaviour of Zn (II) with receptor (1) was investigated by density functional theory (DFT) calculation by using the computer program Gaussian 05 W [38]. All the



a



b



c

**Fig. 3** a Benesi-Hildebrand plot of  $1/\Delta F$  versus  $1/[G]$ ; b Scatchard plot of  $\Delta F/[G]$  versus  $\Delta F$ ; c Connor's plot of  $(1-F/F_0)/[G]$  versus  $F/F_0$

DFT calculations were performed in the gas phase by applying the B3LYP (Becke's three parameter hybrid functional using the LYP correlation functional) using the 6-31G (d, p) basic set (for C, H, N, O atoms of Receptor (1)). The optimized structures of receptor (1) and its complex with Zn (II) are shown in Fig. 5. The receptor (1) has shown non planar geometry in which two arms are in different plane. After addition of Zn (II) ion it showed change in geometry, two arms gets arranged in such way that two Zn (II) ion formed complex with receptor (1). The energy of optimization of receptor (1) and its complex with Zn (II) are  $-1368.9727 \text{ a.u}$  and  $-$

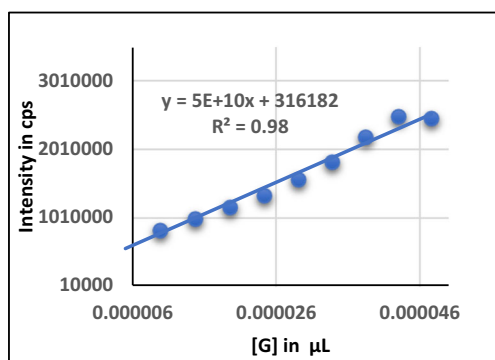


**Fig. 4** Fluorescence intensity receptor (1) ( $2 \text{ ml } 10^{-5} \text{ M}$ ) versus of  $\mu\text{L}$  of Zn (II) ion (G) solution added

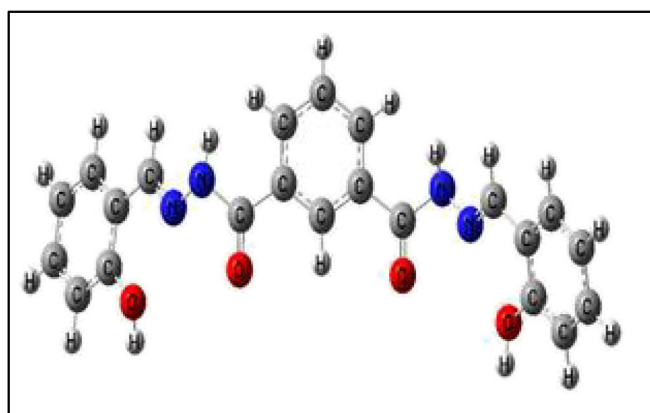
4926.6843 a.u. respectively. Decrease in energy of optimization represents change in geometry and formation of complex resulting increase in stability.

## Electrochemistry

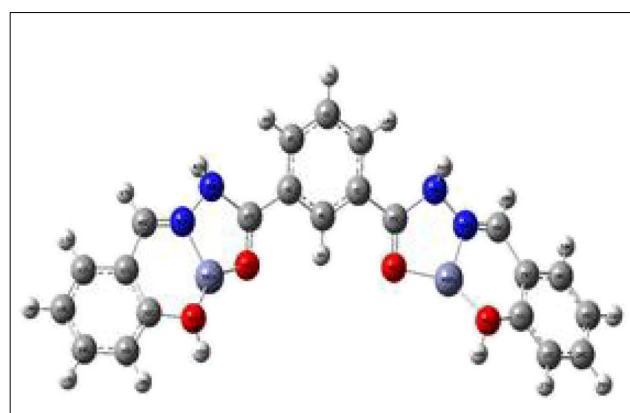
Reorganization behaviour of Receptor (1) was evaluated using electrochemical method in an aqueous medium [39]. Modulation was observed in electrochemical profile of Receptor (1) upon addition of Zn (II) ion (1 equivalent). As shown in Fig. 6, increase in oxidation potential peak with small change from 1.4840 V to 1.4885 V and reduction potential peak of Receptor (1) decreased from  $-1.0858 \text{ V}$  to  $-1.0980 \text{ V}$  respectively after the addition of Zn (II) ion (1 equivalent). This supports that complex formation of Receptor (1) with Zn (II) ion does not change electrochemical structure of Receptor (1) and forms a stable complex with Zn (II).

## Proposed Binding Mechanism

Based on the obtained results of the fluorescence titration and Job's plot, we hereby propose the most probable binding



**a) Receptor (1)**



**b) Receptor (1) and its complex with Zn (II)**

**Fig. 5** The DFT optimized structure **a)** receptor (1) and **b)** Receptor (1) and its complex with Zn (II) calculated B3LYP/6-31G level. The dark grey, grey, red, blue and violet sphere refer for C, H, O, N and Zn atoms respectively

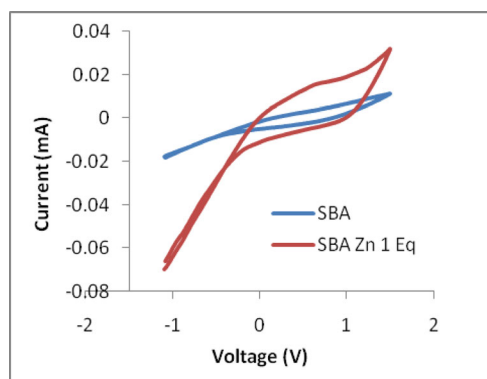


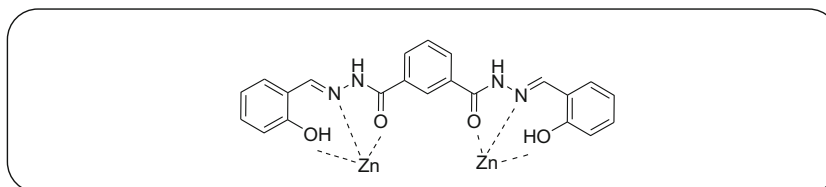
**Fig. 6** Cyclic voltammogram of receptor (1) i.e SBA and its complex with Zn (II) at scan rate of  $50 \text{ mVs}^{-1}$

mode of Receptor (1) with Zn (II) ion shown in Scheme 2. Enhancement in fluorescence intensity of receptor (1) with addition of Zn (II) ion is explained in terms of the operation of a photo-induced electron transfer (PET) mechanism. The formation of complex between receptor (1) with Zn (II) ion is facilitated by the imine group, C = N group, hydroxyl oxygen group which possess binding affinity with many transition metals. In metal free form, receptor (1) experiences PET from imine  $-\text{N}$  and hydroxyl- OH from salicylaldehyde, thus partially quenching its fluorescence. Upon binding of Zn (II) ion with receptor (1), there is a chelation between the metal ion and N of the C = N group and O of the hydroxyl group, PET process is suppressed, leading to an enhancement in fluorescence intensity.

## Conclusions

In conclusion, we have synthesized selective and sensitive receptor i.e. receptor (1) for the detection of Zn (II). The detection of Zn (II) gave rise to increase in fluorescence

**Scheme 2** Propose the binding mechanism of Receptor (1) with Zn (II) ion



intensity. Furthermore, the receptor (1) was not affected by the common interference of other ions like  $\text{Ag}^+$ ,  $\text{Al}^{3+}$ ,  $\text{Ca}^{2+}$ ,  $\text{Cd}^{2+}$ ,  $\text{Co}^{2+}$ ,  $\text{Cu}^{2+}$ ,  $\text{Fe}^{3+}$ ,  $\text{Hg}^{2+}$ ,  $\text{K}^+$ ,  $\text{Mg}^{2+}$ ,  $\text{Na}^+$  and  $\text{Ni}^{2+}$ . The 1:2 binding stoichiometry was established from the Job's plot and the binding constant value was obtained from Benesi-Hildebrand, Scatchard and Connor's plot were found to be  $1.00 \times 10^4 \text{ M}^{-1}$ ,  $1.05 \times 10^4 \text{ M}^{-1}$  and  $1.05 \times 10^4 \text{ M}^{-1}$  respectively. The limit of detection (LOD) and limit of quantification (LOQ) of receptor (1) with Zn (II) ions were  $0.292 \mu\text{M}$  and  $0.974 \mu\text{M}$  respectively. Decrease in energy of optimization of complex represents change in geometry and increase in stability. Electrochemical profile of Receptor (1) and its complex with Zn (II) also supports formation of stable complex. These results clearly demonstrate that our proposed receptor could be useful for analysis of Zn (II) ion in aqueous medium.

## References

- Lehn JM (1995) *Supramolecular chemistry: concepts and perspectives*. Wiley-VCH, Weinheim
- Gale PA (2001) Anion receptor chemistry highlights from 1999. *Coord Chem Rev* 213:79–128. [https://doi.org/10.1016/S0010-8545\(00\)00364-7](https://doi.org/10.1016/S0010-8545(00)00364-7)
- Valeur B et al (Eds.) (2001) *New trends in fluorescence Spectroscopy\_ applications to chemical and life sciences*, Part of the Springer Series on Fluorescence book series (SS FLUOR, volume 1)
- de Silva AP, Gunaratne HQN, Gunnlaugsson T, Huxley AJM, McCoy CP, Rademacher JT, Rice TE (1997) Signaling Recognition Events with Fluorescent Sensors and Switches. *Chem Rev* 97:1515–1566. <https://doi.org/10.1021/cr960386p>
- de Silva AP et al (2000) Combining luminescence, coordination and electron transfer for signalling purposes. *Coord Chem Rev* 205:41–57. [https://doi.org/10.1016/S00108545\(00\)00238-1](https://doi.org/10.1016/S00108545(00)00238-1)
- Que EL, Domaille DW, Chang CJ (2008) Metals in neurobiology: probing their chemistry and biology with molecular imaging. *Chem Rev* 108(5):1517–1549. <https://doi.org/10.1021/cr078203u>
- Frederickson CJ, Suh SW, Koh J-Y, Cha YK, Thompson RB, LaBuda CJ, Balaji RV, Cuajungco MP (2002) Depletion of intracellular zinc from neurons by use of an extracellular Chelator in vivo and in vitro. *J Histochem Cytochem* 50(12):1659–1662. <https://doi.org/10.1177/002215540205001210>
- Stewart AJ, Blindauer CA, Berezenko S, Sleep D, Sadler PJ (2003) Interdomain zinc site on human albumin. *PNAS* 100(7):3701–3706. <https://doi.org/10.1073/pnas.0436576100>
- Perales-Calvo J, Lezamiz A, Garcia-Manyes S (2015) The Mechanochemistry of a Structural Zinc Finger. *J Phys Chem Lett* 6(17):3335–3340. <https://doi.org/10.1021/acs.jpcclett.5b01371>
- Xing G, DeRose VJ (2001) Designing metal-peptide models for protein structure and function. *Curr Opin Chem Biol* 5:196–200. <https://europepmc.org/abstract/med/11282347>. Accessed Mar 2018
- Lim NC, Freake HC, Bruckner C (2004) Illuminating zinc in biological systems. *Chem Eur J* 11:38–49. <https://www.ncbi.nlm.nih.gov/pubmed/15484196>. Accessed Mar 2018
- Prasad AS (2008) Zinc in human health: effect of zinc on immune cells. *Mol Med* 14(5–6):353–357. <https://www.ncbi.nlm.nih.gov/pmc/articles/PMC2277319/>. Accessed Mar 2018
- Folin M, Contiero E, Vaselli GM (1994) Zinc content of normal human serum and its correlation with some hematic parameters. *Biometals* 7(1):75–79. <https://doi.org/10.1007/BF00205198>
- Shankar AH, Prasad AS (1998) Zinc and immune function: the biological basis of altered resistance to infection. *Am J Clin Nutr* 68(suppl):447S–463S. <https://www.ncbi.nlm.nih.gov/pubmed/9701160>. Accessed Mar 2018
- WHO (2003) Zinc in drinking-water. Background document for preparation of WHO guidelines for drinking-water quality. World Health Organization (WHO/SDE/WSH/03.04/17), Geneva
- U.S. EPA, (May 2009) National Primary Drinking Water Regulations. <http://www.epa.gov/safewater/ki.PDF>. Accessed Mar 2018
- Prasad AS (1998) Zinc and immunity. *Mol Cell Biochem* 188:63–69. <https://www.ncbi.nlm.nih.gov/pmc/articles/PMC2277319/>. Accessed Mar 2018
- Bush AI, Tanzi RE (2002) The galvanization of  $\beta$ -amyloid in Alzheimer's Disease. *PNAS* 99(11):7317–7319. <https://doi.org/10.1073/pnas.122249699>
- Larson AA, Kitto KF (1998) *J Pharmacol Exp Ther* 288(2):759–765. <http://jpet.aspetjournals.org/content/288/2/759.short>. Accessed Mar 2018
- Dansch G, Stoltenberg M (2005) Zinc-specific autometallographic in vivo selenium methods: tracing of zinc-enriched (ZEN) terminals, ZEN pathways, and pools of zinc ions in a multitude of other ZEN cells. *J Histochem Cytochem* 53(2): 141–153. <https://doi.org/10.1369/jhc.4R6460.2005>
- Yörük İ, Deger Y, Mert H, Mert N, Ataseven V (2007) Serum Concentration of Copper, Zinc, Iron, and Cobalt and the Copper/Zinc Ratio in Horses with Equine Herpesvirus-1. *Biol Trace Elem Res* 118:38–42. <https://doi.org/10.1007/s12011-007-0023-y>
- Bitanihirwe BKY, Cunningham MG (2009) Zinc: The Brain's Dark Horse bitanihirwe. *SYNAPSE* 63:1029–1049. <https://doi.org/10.1002/syn.20683>
- Zatta P, Drago D, Bolognin S, Sensi SL (2009) Alzheimer's disease, metal ions and metal homeostatic therapy. *Trends Pharmacol Sci* 30(7):346–354. <https://doi.org/10.1016/j.tips.2009.05.002>
- Li W, Wang J, Zhang J, Wang W (2015) Molecular simulations of metal-coupled protein folding. *Curr Opin Struct Biol* 30:25–31. <https://doi.org/10.1016/j.sbi.2014.11.006>
- Burdette SC, Walkup GK, Spingler B, Tsien RY, Lippard SJ (2001) Fluorescent sensors for  $\text{Zn}^{2+}$  based on a fluorescein platform: synthesis, properties and intracellular distribution. *J Am Chem Soc* 123:7831–7841. <https://doi.org/10.1021/ja010059j>
- Maruyama S, Kikuchi K, Hirano T, Urano Y, Nagano T (2002) A novel, cell-permeable, fluorescent probe for Ratiometric imaging of

- zinc ion. *J Am Chem Soc* 124:10650–10651. <https://doi.org/10.1021/ja026442n>
27. Callan JF, de Silva AP, Magri DC (2005) Luminescent sensors and switches in the early 21st century. *Tetrahedron* 61(36):8551–8588. <https://doi.org/10.1016/j.tet.2005.05.043>
  28. Lee DY, Singh N, Kim MJ, Jang DO (2010) Ratiometric fluorescent determination of Zn(II): a new class of tripodalreceptor using mixed imine and amide linkages. *Tetrahedron* 66(2010):7965–7969. <https://doi.org/10.1016/j.tet.2010.08.024>
  29. Lukowiak B, Vandewalle B, Riachy R, Kerr-Conte J, Gmyr V, Belaich S, Lefebvre J, Pattou F (2001) Identification and purification of functional human beta-cells by a new specific zinc-fluorescent probe. *J Histochem Cytochem* 49(4):519–528. <https://www.ncbi.nlm.nih.gov/pubmed/11259455>. Accessed Mar 2018
  30. Nimmanon T, Ziliotto S, Morris S, Flanagan L, Taylor KM (2017) Phosphorylation of zinc channel ZIP7 drives MAPK, PI3K and mTOR growth and proliferation signalling. *Metallomics* 9:471–481. <https://www.ncbi.nlm.nih.gov/pubmed/28205653>. Accessed Mar 2018
  31. Aulsebrook ML, Graham B, Grace MR, Tuck KL (2014) The synthesis of luminescent lanthanide-based chemosensors for the detection of zinc ions. *Tetrahedron* 70(29):1–6. <https://doi.org/10.1016/j.tet.2014.04.078>
  32. Song EJ, Park GJ, Lee JJ, Lee S, Noh I, Kim Y, Kim S-J, Kim C, Harrison RG (2015) A fluorescence sensor for Zn<sup>2+</sup> that also acts as a visible sensor for Co<sup>2+</sup> and Cu<sup>2+</sup>. *Sensors Actuators B Chem* 213(5):268–275. <https://doi.org/10.1016/j.snb.2015.02.094>
  33. Stuart Tobias R (1958) The determination of stability constants of complex inorganic species in aqueous solutions. *J Chem Educ* 35(12):592–599. <https://doi.org/10.1021/ed035p592>
  34. Benesi HA, Hildebrand JH (1949) A spectrophotometric investigation of the interaction of iodine with aromatic hydrocarbons. *J Am Chem Soc* 71(8):2703–2707. <https://doi.org/10.1021/ja01176a030>
  35. Scatchard G (1949) The attractions of Proteins for small molecules and ions. *Ann N Y Acad Sci* 51:660–672. <https://doi.org/10.1111/j.1749-6632.1949.tb27297.x>
  36. Connors KA (1932) The measurements of molecular complex stability. Wiley, New York, p c1987
  37. MacDougall D, Crummett WB et al (1980) Guidelines for Data Acquisition and Data Quality Evaluation in Environmental Chemistry. *Anal Chem* 52:2242–2249. <https://doi.org/10.1021/ac50064a004>
  38. Frisch MJ, Trucks GW, Schlegel HB et al (2004) Gaussian 03, revision C.02. Gaussian Inc, Wallingford CT
  39. Santos-Figueroa LE, Moragues ME, Manuela M, Raposo M et al (2012) Synthesis and evaluation of thiosemicarbazones functionalized with furylmoieties as new chemosensors for anion recognition org. *Biomol Chem* 10:7418–7428. <https://doi.org/10.1039/c2ob26200b>

**Publisher's Note** Springer Nature remains neutral with regard to jurisdictional claims in published maps and institutional affiliations.